



**Preliminary Estimates of Dose and Residual Activation of
Selected Components in Ring Collimation Straight**

BNL/SNS TECHNICAL NOTE

NO. 077

H. Ludewig, J. Walker*, N. Catalan-Lasheras, N. Simos,
A. Mallen, J. Wei, and M. Todosow

June 6, 2000

COLLIDER-ACCELERATOR DEPARTMENT
BROOKHAVEN NATIONAL LABORATORY
UPTON, NEW YORK 11973

PRELIMINARY ESTIMATES OF DOSE AND RESIDUAL ACTIVATION OF SELECTED COMPONENTS IN RING COLLIMATION STRAIGHT

H. Ludewig, J. Walker*, N. Catalan-Lasheras, N. Simos, A. Mallen, J. Wei, and M. Todosow.
Brookhaven National Laboratory, Upton, New York, USA. 11973.

Introduction

In this report an estimate of the dose to the following components in the collimation straight of the ring will be made:

- 1) Windings of the quadru-pole magnets,
- 2) Windings of a typical corrector magnet,
- 3) Cable located along the inside tunnel wall, and
- 4) Outer edge of the earth berm covering the tunnel.

In addition, to the above dose estimates the residual activation of the following components in the collimation straight following machine operation and shutdown, will be made:

- 1) Tunnel cooling water,
- 2) Tunnel air,
- 3) Cooling water for the collimators, and
- 4) Windings and pole pieces of a typical quadru-pole.

The estimate of activation will be made primarily to determine the concentration of long lived isotopes, and in the case of water and air the concentration of tritium will be of particular interest.

In all the above estimates the machine is assumed to operate at an average power of 2 MW, with a proton energy of 1 GeV, and a loss of 0.001. In the case of the dose estimates it was assumed that the loss occurs at all three collimator locations i.e. 0.001 at the first, 0.001 at the second, and finally 0.001 at the third. If the loss profile is different the dose components due to losses at the various collimators can be added in different proportions. In the case of the residual activation estimates the loss was simulated only at the first collimator. A residual activation estimate corresponding to a more realistic loss profile will be carried out when the losses are more clearly defined. In these estimates the entire collimation straight will be simulated, including the primary scraper/collimator, the other two collimators, two doublets (consisting of two quadru-poles of unequal length), two quadru-poles at either end, and one corrector magnet positioned in the most vulnerable position (between the first doublet and the scraper/collimator). Four cable trays are positioned along the inner wall at a variety of elevations above the vacuum chamber. Two tunnel cooling water lines are considered, one along the inside wall of the tunnel, and the second along the outside wall below the crane.

In the following sections the model and method of analysis will be described, dose estimates will

be presented and finally the residual activation results will be presented.

Methods and Modeling

The above estimates of dose and residual activation are both based on the MCNP family of codes. In the case of the dose estimate the MCNPX [1] code was used. This code uses the combinatorial representation of geometry, in the same way all previous MCNP based codes have used it, and the geometry descriptions are inter-changeable among all codes. However, MCNPX has a high energy transport section available, which allows the same physical phenomena as the LAHET code [2]. The primary proton (1 GeV), and all the resulting secondary particles can be followed, edited and tallied in any desirable manner over the entire energy range of interest.

In order to estimate the dose in a particular cell the energy deposition was estimated in that cell (F6:n,p,h tally in MCNPX) in MeV/g-proton. In order to convert MeV/g to rad it is recognized that 1 rad=100 erg/g, and that there are 1.602×10^{-6} ergs/MeV. Thus the F6 tally was multiplied by 1.602×10^{-8} to result in rad/proton. This value was then further multiplied by the loss in protons/s (1.243×10^{13}), seconds/hr (3600), and mrad/rad (1000). The total multiplicative factor for the F6 tally is thus 7.168675×10^{11} to result in a dose of mrad/hr in a particular cell of interest.

Due to the need to link to other codes the residual activation estimate was made using the LAHET codes for particles above 20 MeV; and MCNP [3] for particles below 20 MeV. In addition, a suitably modified version of the ORIGEN [4] code was used to estimate the buildup of spallation products during machine operation, and their decay following shutdown. In this calculational string the spallation product mass distribution is determined by the LAHET code, the averaged neutron energy spectrum in the cell of interest is determined by MCNP, and these two pieces of information are used to determine the appropriate nuclear cross section data and inventory of spallation products used in the modified ORIGEN code for the estimated build-up and decay of radioactive nuclides in the cell while the machine is operating and following shutdown. In this case the machine loss rate in protons/s (1.243×10^{13} protons/s lost on primary scraper) is used to determine the neutron flux, and is thus the connection to the overall machine power. In addition assumptions must be made regarding the operating time of the machine. In all these estimates it was assumed that the machine operates at full power for 180 days. In order to determine the residual activation for different times it is reasonable to scale the activity by the number of full power days. The two calculational sequences described above are shown in Fig. 1. The upper sequence represents the determination of dose using MCNPX, and the lower sequence represents the determination of residual activation. It is seen that the lower sequence involves several codes, and an extensive nuclear data library.

The actual layout of the lattice in the collimation straight of the ring is shown in Fig. 2. From the figure it is seen that the straight section is 30 m in length, with three collimators, two sets of doublets, two quadru-poles one at each end, and two corrector magnets. The distance between the quadru-poles and the two collimators at each end is approximately 1.5 m, and the distance from the primary scraper/collimator to the corrector magnet is approximately 0.5 m. This short distance between magnets and high loss locations in the ring raises the concern of radiation induced damage to these components, in particular the insulation of the magnet windings. In

addition, the potential radiation damage to the insulation of the cables located in the cable trays attached to the inner wall above the collimators will be of concern. There is a comparatively long straight section between the second collimator and the second doublet (~ 12 m.) Which ensures that these magnets should not be subject to the same environment as the first doublet.

The primary scraper/collimator consists of a 0.55 cm thick platinum scraper which protrudes into the halo, and perturbs the beam orbit sufficiently that the particles are deflected into one of the secondary collimators. It has been found that the scraper location must be surrounded by a substantial structure to absorb the bulk of the secondary particles generated in the scraper due to nuclear interactions, and tertiary particles generated in the structure. A fraction of this particle shower leaks out, and irradiates the down stream magnets. In these estimates it was assumed that the vacuum chamber remains unchanged in size, thus resulting in a substantial leakage path for secondary particles leaving the scraper. The second and third collimators are restrictions in the vacuum chamber and follow the beam profile at that particular location.

Dose Estimates

Estimates of the dose were carried out for selected magnet cells for each magnet, cable located in trays closest to the collimators and the outer cells of the earth berm.

Magnets

Dose estimates were carried out for the section of the magnet windings protruding from the magnet frame. Thus there are four cells on each side of a quadru-pole magnet. This is illustrated in Figs. 3 and 4, which show a cross section through a typical quadru-pole and the location of the four cells of interest. The MCNP model is illustrated in Fig 5, which shows the three collimators, two doublets, two quadru-poles and one corrector. The corrector is the one located closest to the primary scraper/collimator and is expected to experience a high dose. The estimated doses for the various magnets are shown on table 1 for the loss pattern described above. Briefly, it was assumed that the same loss is experienced at each collimator. The assumed loss is 0.001 of the primary beam at full power. The resulting dose is the sum of the dose estimated for losses at each collimator. The first quadru-pole experiences a comparatively low dose, approximately 3 rad/hr on the side opposite the collimator, and approximately 50 rad/hr on the side facing the collimator. The corrector magnet volumes experience doses varying from 2000 rad/hr - 4000 rad/hr depending on location, and the attached doublet experience doses between 4000 rad/hr - 5000 rad/hr. This combination experiences the highest dose, since it is comparatively close to the primary scraper/collimator. Cells in the second doublet have doses which are between 150 rad/hr - 250 rad/hr, and finally cells in the last quadru-pole experience doses between 515 rad/hr - 620 rad/hr.

The life expectance of kapton (proposed insulation for the magnet windings) in a radiation field is between 5×10^8 rad - 10^9 rad, thus at the highest dose rate the magnet insulation should last approximately 10^5 hrs - 2×10^5 hrs. If it assumed that the machine will operate for three quarters of a year it should be expected that the first doublet will have to be changed at least once in the machine lifetime - assuming a thirty year life.

Cable

The cable tray is assumed to be located along the inside wall of the ring, at an elevation just above the height of the collimator diameter (1 m above the vacuum chamber centerline). This arrangement is illustrated in Fig.6, which shows four cable trays fixed to the inside tunnel wall above the collimators. The cell numbers refer to the lower cable tray, closest to the collimators and vacuum chamber, and their ordered increases with distance from the entrance to the collimation straight of the ring. As with the magnets the final dose was assumed to be due to an equal loss at each collimator. The results shown in Table 1 show that the dose varies axially along the tunnel, with the highest dose occurring just downstream of the primary scraper/collimator. It is seen that the dose varies between 125 rad/hr - 1525 rad/hr. Although this dose is lower than that experienced by the magnet windings, the insulation on cables is generally not as resistant to radiation damage as the insulation on magnet windings. If the insulation can withstand between 10^8 rad - 5×10^8 rad the cables should last approximately 7×10^4 hrs - 4×10^5 hrs. This lifetime estimate would suggest that at least a section of the cable might have to be replaced during the lifetime of the machine.

Earth berm and tunnel air

The dose estimated in the earth berm and selected tunnel air cells, as a result of losses at the collimators is also shown in Table 1. The earth berm thickness assumed in this analysis is 5 m, and the composition is characteristic of soil at ORNL (same as soil used in LINAC earth berm calculation). The cells being considered for this estimate are shown on Fig. 6. In the case of the earth berm only those cells located on the outside of the berm on either side of the tunnel were considered. The distribution of dose within the berm was not estimated. The results indicate that there is a pronounced variation along the outside of the berm, both on the inside and outside of the tunnel. The dose is quite low at the entrance cells ($\sim .05$ mrad/hr), and then increases to approximately 4.2 mrad/hr just downstream of the primary scraper/collimator location, and then drops down again. However, at the exit of the collimation straight the dose is still ~ 0.8 mrad/hr. Since, the losses along the collimation straight are expected to be higher than the nominally assumed 1 W/m a thicker earth berm should be investigated for this region.

The dose to the tunnel air was estimated for the five cells shown on Fig. 7. The dose peaks downstream of the scraper/collimator, with a peak value of ~ 500 rad/hr.

It should be noted that the above dose estimates were based on the nominal loss rate assumed for collimators (0.001 of the full power operating beam current). If the losses are higher for any reason, then the doses will increase proportionally, and the conclusions regarding component lifetime should be modified accordingly.

Residual Activity

An estimate was made of the residual activity in the collimator cooling water, tunnel cooling water, selected magnet cells, and the tunnel atmosphere. These estimates were made assuming that the losses are confined to the primary scraper/collimator, additional activity due to other

losses have not been estimated at this time. However, based on the above results, losses at this location are responsible for a significant fraction of the dose to the magnets, cables, and earth berm, and it is thus expected that the estimates of activity based on losses at this location should capture a significant fraction of their activity. The primary purpose of this preliminary estimate is to determine the residual activation due to nuclides which survive beyond approximately 4 hours following machine shutdown. In all cases it is assumed that the machine operates at full power (2 MW) for 180 days, and then the residual activation is determined immediately following shutdown, 4 hrs later, and at a selection of times beyond that period.

Collimator cooling water.

Activation of the cooling water in the four major volumes in the primary collimator was estimated for the operating cycle summarized above. Two of these volumes are situated on either side of the scraper, and thus experience the scattered primary proton and secondary proton and neutron fluxes. The other two volumes are situated at either end of the collimator structure and thus are exposed primarily to neutron fluxes, the protons being stopped by the collimator.

The results of these estimates in curies are shown on Tables 2 - 4. The results on Table 2 show that the cells closest to the scraper have the highest residual activity, which dies off quite rapidly as the shorter lived isotopes decay. Immediately following shutdown the activity is dominated by ^{15}O , ^{16}N , ^{11}C , and ^{12}B , all of which have a short half-life. Following 4 hrs. the dominant nuclides are ^7Be , and ^{14}C , in selected cases ^3H and ^{10}Be also play a role. ^3H is generated in all cells. The resulting gamma-ray source is shown in Table 3. The source essentially follows the activity variation, being highest immediately following shutdown, and decreasing precipitously following 4 hrs after shutdown. After one day the source remains largely constant, being caused primarily by the decay of ^7Be and ^{14}C . A detail accounting of the activity due to ^3H , ^7Be , ^{10}Be , and ^{14}C is shown on Table 4. It is seen that the production of these isotopes occurs in the volumes closest to the scraper. The total activity of these nuclides in these volumes are:

Isotope Activity (Curies)	
Tritium	2.6×10^{-8}
Beryllium-7	6.1×10^{-2}
Carbon-7	2.2×10^{-5}

Selected magnet volumes in first Doublet

The quadru-pole magnets and the associated corrector magnet experience the highest doses of any component in the collimation straight of the ring. Based on this data it was decided to estimate the residual activity in that portion of the windings that protrude beyond the magnet frame. This should be considered an initial estimate, a more detailed analysis will be used to estimate the residual dose which can be expected in the event that such a magnet needs to be changed. The residual activity in Curies is shown in Table 2. It is seen that the initial activity, immediately following shutdown is less than one Curie, and then it drops off by approximately a factor of 5 after 4 hrs. The subsequent drop-off is not as rapid. The gamma-ray source (in

photons/s) as a function of time and cell number is shown on Table 3. It is seen that the source is approximately 3.5×10^{10} photons/s immediately after shutdown, but then drops off by approximately an order of magnitude following 4 hrs. As with the activity, the variation following 4 hrs is much slower, and even following 30 days there is a significant source. Immediately after shutdown the activity is dominated by isotopes of copper, nickel, iron, manganese, vanadium, cobalt, oxygen, carbon, and aluminum. The short lived isotopes decay within the 4 hr period and the activity is then dominated by ^{63}Ni , ^{60}Co , ^{58}Co , ^{57}Co , ^{56}Co , ^{55}Fe , ^{54}Mn , ^{14}C , and ^{10}Be . The production of tritium in the cooling water is extremely small (approximately 10^{-15} Curies per cell), and a more accurate value will have to be determined at a later date.

Tunnel Atmosphere

An estimate of the tunnel atmosphere was made at several locations along the tunnel shown in Fig 7. Nitrogen, oxygen, hydrogen, and argon were included in the description of the atmosphere. Immediately following shutdown the activity is dominated by ^{13}N , ^{37}Ar , ^{39}Cl , and ^{16}N . Following 4 hrs the activity is dominated by ^{14}C , and in selected cells ^{10}Be . ^3H is generated in all cases, but in extremely small quantities. The gamma-ray source is dominated by the presence of ^{14}C . A detailed accounting of the long lived isotopes indicates that the inventories are:

Isotope	Activity (Curies)
Tritium	1.0×10^{-10}
Beryllium-7	1.4×10^{-9}
Carbon-7	1.1×10^{-3}

In a real atmosphere the air would likely be circulated and vented following an appropriate hold-up to ensure that the short lived isotopes have decayed. In this manner the build-up of activity will be limited by the time the air is exposed to the implied radiation environment. In the above estimates the exposure time was 180 days.

Tunnel cooling water

The location of the tunnel cooling water line has not been fixed yet. Thus two locations were investigated for this estimate. In the first case it is assumed that the cooling pipe runs along the inside tunnel wall, at essentially floor level, and in the second case it is assumed the cooling pipe runs along the outside tunnel wall and is suspended approximately 1.5 m below the ceiling. These arrangements are shown in Fig. 6. Several cells on either side of the scraper/collimator were used to estimate the activity. The results shown on Table 2 indicate that the activity immediately following shutdown is dominated by ^{15}O , ^{16}N , and ^7Be in selected cells. Following 4 hrs the activity is dominated by ^{14}C and ^7Be in selected cells. Of the two locations considered for the cooling water line, the one along the outside wall below the ceiling has a total activity significantly lower than that of a line located along the inside wall just above the floor. The final location of the cooling line will have to satisfy additional constraints such as ease of connecting to machine components, ease of shielding if necessary, and ease of maintenance. The total

inventory of relatively long lived isotopes for the two locations are given below:

Nuclide	Along inside wall (Curies)	Along outside wall (Curies)
Tritium	4.2×10^{-10}	4.1×10^{-11}
Beryllium-7	2.4×10^{-3}	1.5×10^{-3}
Beryllium-10	3.6×10^{-10}	~
Carbon-14	4.0×10^{-7}	4.0×10^{-7}

The above estimates will have to be updated to include additional losses along the collimation straight, the total inventory of the cooling water loop, and the flow velocity (which determines the duration of the water will spend in a potentially high loss section of the ring).

Conclusions

The following conclusions can be drawn from this study:

- 1) The results reported in this study are a strong function of the assumptions regarding loss, average power and full power operating time,
- 2) In this study it was assumed that the loss is 0.001 of the beam on the face of each of the collimators, the accelerator operated at an average power of 2 MW in an un-interrupted fashion for 180 days. The effect of any variation from these assumptions can be obtained by scaling (within limits), and
- 3) Once a firm design is established these estimates can be repeated for realistic loss patterns, operating profiles, and power levels.

References

- 1) *MCNPX Users Manual - Version 2.1.5*, L.S. Waters, ed., Los Alamos National Laboratory, Los Alamos, NM, TPO-E83-G-UG-X-00001 (1999)
- 2) R.E. Prael and H. Lichtenstein, "*User Guide to LCS: The LAHET Code System*", Los Alamos National Laboratory, Los Alamos, NM, LA-UR-89-3014 (1989).
- 3) *MCNP-A General Monte Carlo N-Particle Transport Code Version 4A*, J.F. Breisemeister, ed., Los Alamos National Laboratory, Los Alamos, NM, LA-12625-M (1993).
- 4) A.G. Croff, "*ORIGEN2 - A Revised and Updated Version of the Oak Ridge Isotope Generation and Depletion Code*", Oak Ridge National Laboratory, Oak Ridge, TN, ORNL-5621 (1980).

TABLE 2 - ACTIVATION BY CELL IN CURIES

Cell number	Shutdown	4 hrs	1 day	7 days	30 days	Remarks
10	2.202(-4)	4.0(-7)	4.0(-7)	4.0(-7)	4.0(-7)	
11	4.270(-1)	1.821(-2)	1.8(-2)	1.655(-2)	1.234(-2)	Primary Collimator
12	1.027(0)	4.249(-2)	4.2(-2)	3.884(-2)	2.879(-2)	Cooling Water
13	8.55(-2)	1.604(-2)	1.604(-2)	1.604(-2)	1.604(-2)	
32	2.051(-4)	1.562(-4)	1.562(-4)	1.562(-4)	1.562(-4)	
34	2.423(-2)	4.703(-4)	4.703(-4)	4.703(-4)	4.703(-4)	Tunnel Air
3003	3.296(-2)	3.77(-3)	3.547(-3)	3.188(-3)	2.149(-3)	
4065	7.058(-3)	8.852(-5)	8.852(-5)	8.852(-5)	8.852(-5)	
458	3.683(-3)	9.447(-11)	9.447(-11)		1.992(-14)	
459	1.816(-2)	9.101(-4)	8.998(-4)	8.322(-4)	6.169(-4)	Tunnel Cooling Water
460	1.664(-2)	1.06(-6)	1.007(-7)	1.007(-7)	1.007(-7)	(along inside wall
461	1.443(-2)	1.516(-3)	1.499(-3)	1.387(-3)	1.028(-3)	and at floor level)
470	4.35(-4)	1.0(-7)	1.0(-7)	1.0(-7)	1.0(-7)	
471	2.629(-3)	1.0(-7)	1.0(-7)	1.0(-7)	1.0(-7)	Tunnel Cooling Water
472	6.018(-3)	4.797(-7)	4.797(-3)	4.797(-7)	4.797(-7)	(along outside wall
473	4.192(-3)	4.797(-7)	4.797(-7)	4.797(-7)	4.797(-7)	and just below crane)
474	7.007(-3)	1.517(-3)	1.517(-3)	1.517(-3)	1.517(-3)	
1048	6.78(-1)	1.80(-1)	9.871(-2)	6.807(-2)	5.647(-2)	
1049	6.031(-1)	1.412(-1)	6.645(-2)	4.031(-2)	3.379(-2)	
1050	6.315(-1)	1.52(-1)	9.1(-2)	6.4(-2)	5.096(-2)	
1051	7.081(-1)	2.473(-1)	1.593(-1)	1.141(-1)	8.693(-2)	
1053	4.840(-1)	8.977(-2)	3.393(-2)	1.211(-2)	8.363(-3)	
1054	4.812(-1)	1.042(-1)	5.454(-2)	3.019(-2)	2.275(-2)	First Doublet
1055	4.411(-1)	8.458(-2)	4.63(-2)	3.229(-2)	2.755(-2)	Windings protruding
1056	5.039(-1)	1.036(-1)	5.8(-2)	3.83(-2)	3.18(-2)	beyond magnet -
1248	6.311(-1)	1.249(-1)	5.789(-2)	3.084(-2)	2.595(-2)	front and back
1249	5.366(-1)	1.440(-1)	6.340(-2)	3.467(-2)	2.75(-2)	
1250	6.657(-1)	1.869(-1)	8.932(-2)	5.147(-2)	4.087(-2)	
1251	5.494(-1)	1.549(-1)	1.104(-1)	8.045(-2)	6.172(-2)	
1253	5.172(-1)	1.020(-1)	5.933(-2)	4.086(-2)	3.355(-2)	
1254	5.196(-1)	1.112(-1)	5.729(-2)	3.301(-2)	2.194(-2)	
1255	4.826(-1)	9.767(-2)	4.293(-2)	1.848(-2)	1.519(-2)	
1256	4.585(-1)	1.035(-1)	5.084(-2)	3.086(-2)	2.633(-2)	

TABLE 3 - GAMMA-RAY SOURCE IN PHOTONS/SECOND

Cell number	Shutdown	4 hrs	1 day	7 days	30 days	
10	3.427(7)	4.412(2)	4.412(2)	4.412(2)	4.412(2)	Primary Collimator Cooling Water
11	3.971(10)	8.851(5)	5.737(3)	5.737(3)	5.737(3)	
12	8.517(10)	2.404(6)	1.685(4)	1.685(4)	1.685(4)	
13	6.371(9)	1.846(3)	1.764(3)	1.764(3)	1.764(3)	
32	6.832(6)	1.72(5)	1.72(5)	1.72(5)	1.72(5)	Tunnel Air
34	1.808(9)	5.18(5)	5.18(5)	5.18(5)	5.18(5)	
3003	2.768(9)	1.226(7)	3.0(6)	2.71(6)	1.856(6)	
4065	5.021(8)	9.748(4)	9.748(4)	9.748(4)	9.748(4)	
458	3.418(8)	1.015(1)	~	~	~	Tunnel Cooling Water (along inside wall and at floor level)
459	1.707(9)	3.164(4)	2.206(2)	2.206(2)	2.206(2)	
460	1.667(9)	6.293(4)	1.127(2)	1.127(2)	1.127(2)	
461	6.015(8)	1.103(2)	1.103(2)	1.103(2)	1.103(2)	
470	6.834(7)	1.103(2)	1.103(2)	1.103(2)	1.103(2)	Tunnel Cooling Water (along outside wall and just below crane)
471	2.605(8)	1.103(2)	1.103(2)	1.103(2)	1.103(2)	
472	5.487(8)	3.141(4)	~	~	~	
473	3.511(8)	3.141(4)	~	~	~	
474	4.710(8)	6.305(4)	2.207(2)	2.207(2)	2.207(2)	
1048	3.944(10)	7.255(9)	4.491(9)	3.717(9)	3.064(9)	First Doublet Windings protruding beyond magnet - front and back
1049	4.330(10)	5.972(9)	3.179(9)	2.525(9)	2.1(9)	
1050	4.3(10)	5.471(9)	3.601(9)	2.954(9)	2.44(9)	
1051	4.314(10)	1.207(10)	8.824(9)	6.822(9)	4.749(9)	
1053	2.963(10)	3.922(9)	1.946(9)	1.085(9)	6.046(9)	
1054	3.05(10)	3.225(9)	1.742(9)	1.197(9)	9.572(8)	
1055	2.79(10)	3.3(9)	1.986(9)	1.639(9)	1.381(9)	
1056	3.019(10)	4.079(9)	2.691(9)	2.194(9)	1.79(9)	
1248	3.928(10)	4.042(9)	1.804(9)	1.131(9)	9.857(8)	
1249	3.0(10)	6.014(9)	3.19(9)	2.38(9)	1.511(9)	
1250	4.089(10)	7.716(9)	4.33(9)	3.114(9)	2.353(9)	
1251	3.921(10)	6.678(9)	5.624(9)	4.392(9)	3.06(9)	
1253	3.443(10)	3.624(9)	2.206(9)	1.774(9)	1.494(9)	
1254	3.368(10)	5.332(9)	3.253(9)	1.973(9)	1.034(9)	
1255	2.726(10)	2.975(9)	1.561(9)	1.016(9)	8.341(8)	
1256	2.567(10)	3.86(9)	2.157(9)	1.683(9)	1.419(9)	

TABLE 4 - ACTIVATION IN CURIES OF LONG LIVED ISOTOPES

Cell number	Shutdown	Tritium	Beryllium-7	Beryllium-10	Carbon-14	Remarks
10	2.202(-4)	2.336(-15)	~	~	4.01(-7)	
11	4.270(-1)	5.61(-9)	1.823(-2)	~	5.21(-6)	Primary Collimator
12	1.027(0)	1.952(-8)	4.25(-2)	~	1.5(-5)	Cooling Water
13	8.55(-2)	6.905(-10)	~	~	1.6(-6)	
Total		2.582(-8)	6.073(-2)		2.221(-5)	
32	2.051(-4)	4.221(-18)	~	~	1.562(-4)	
34	2.423(-2)	5.697(-17)	~	7.18(-10)	4.703(-4)	Tunnel Air
3003	3.296(-2)	9.491(-11)	~	7.177(-10)	3.406(-4)	
4065	7.058(-3)	8.892(-12)	~	~	8.852(-5)	
Total		1.038(-10)		1.436(-9)	1.056(-3)	
458	3.683(-3)	2.0(-14)	~	~	~	
459	1.816(-2)	2.168(-10)	9.114(-4)	8.4(-20)	2.0(-7)	Tunnel Cooling Water
460	1.664(-2)	1.17(-10)	~	3.6(-10)	1.0(-7)	(along inside wall
461	1.443(-2)	8.8(-11)	1.52(-3)	~	1.0(-7)	and at floor level)
Total		4.218(-10)	2.431(-3)	3.6(-10)	4.0(-7)	
470	4.35(-4)	2.1(-14)	~	~	1.0(-7)	
471	2.629(-3)	4.05(-11)	~	~	1.0(-7)	Tunnel Cooling Water
472	6.018(-3)	2.369(-14)	~	1.8(-21)	7.1(-16)	(along outside wall
473	4.192(-3)	2.384(-14)	~	1.9(-21)	2.6(-14)	and just below crane
474	7.007(-3)	7.025(-15)	1.52(-3)	9.7(-22)	2.0(-7)	
Total		4.064(-11)	1.52(-3)	4.67(-21)	4.0(-7)	

Figure 1: Calculational method

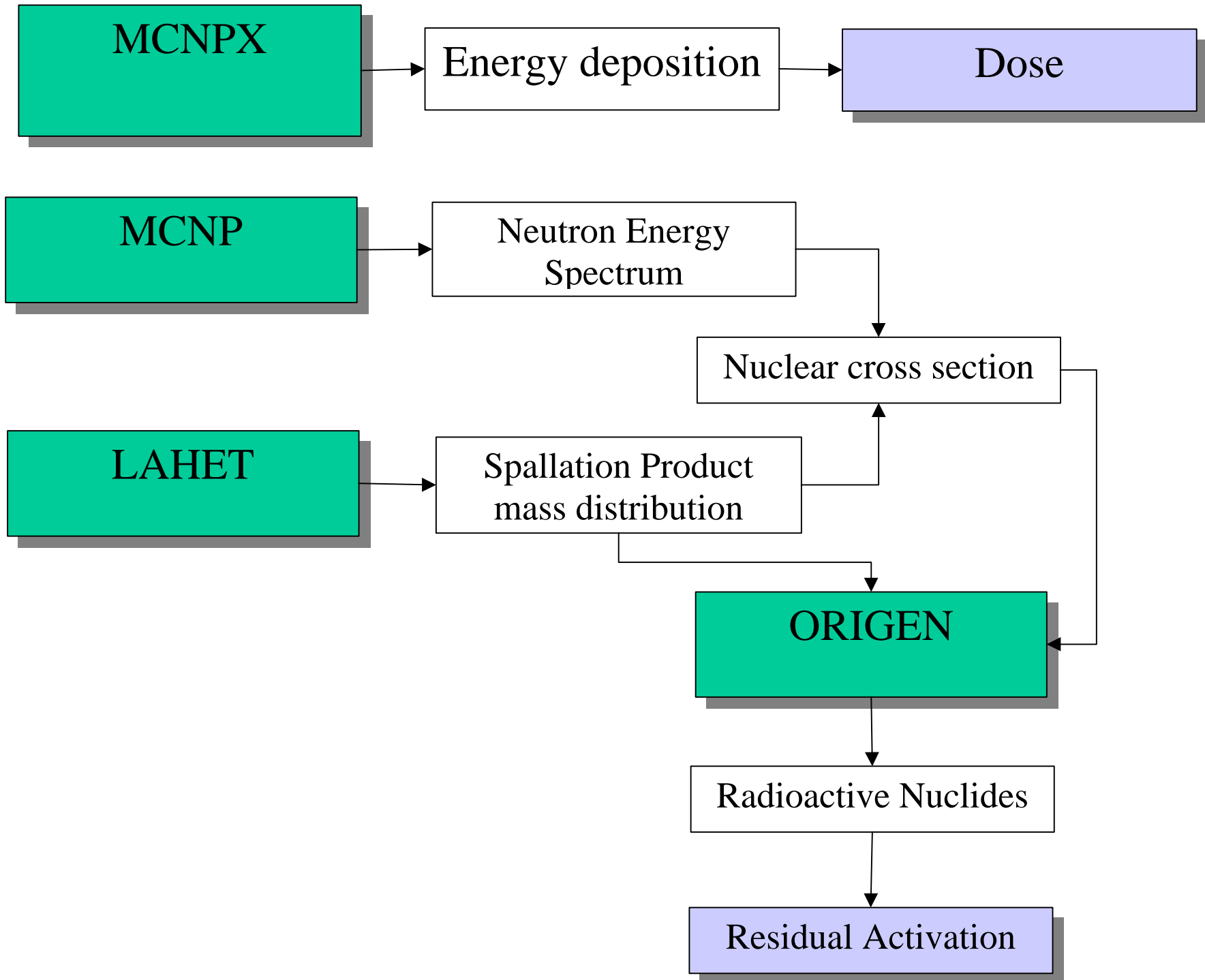
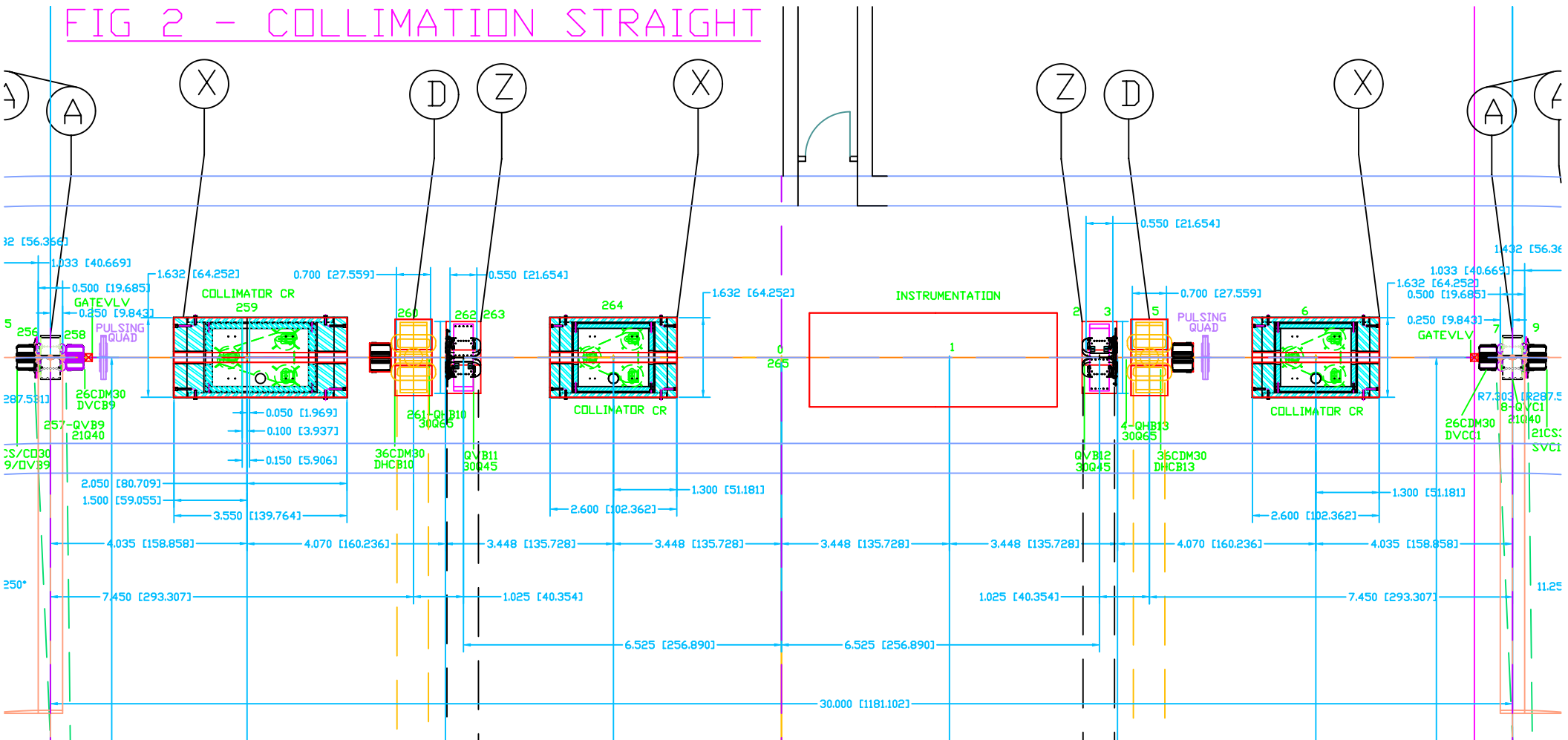


FIG 2 - COLLIMATION STRAIGHT



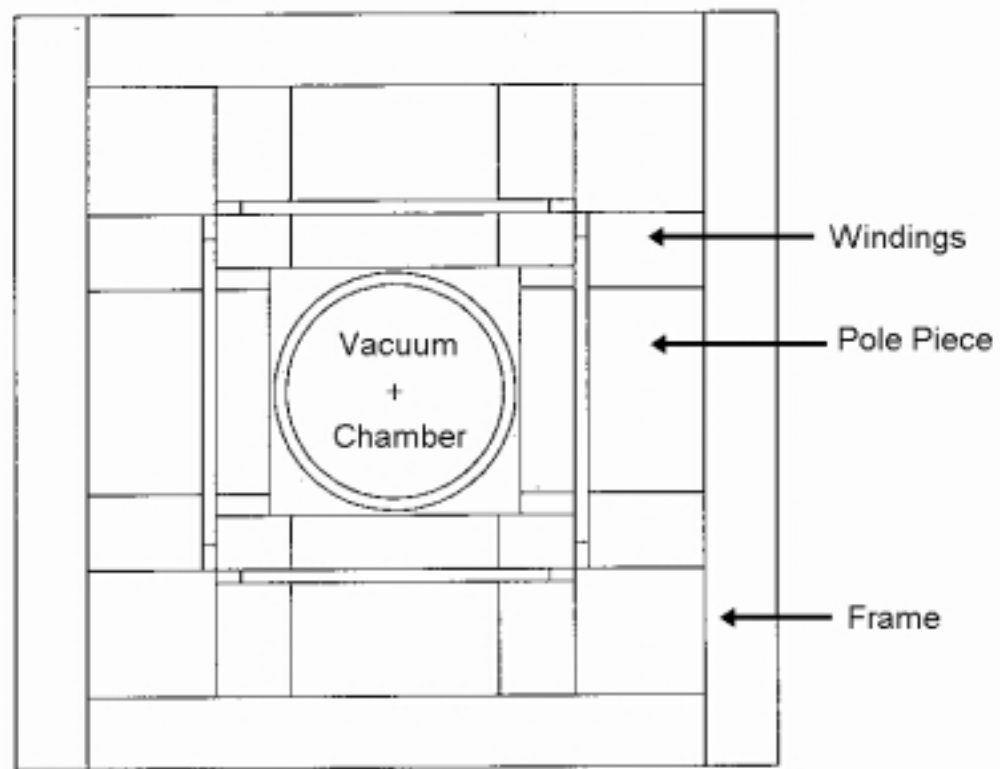


Figure 3: Cross Section Through Quadru-Pole Magnet

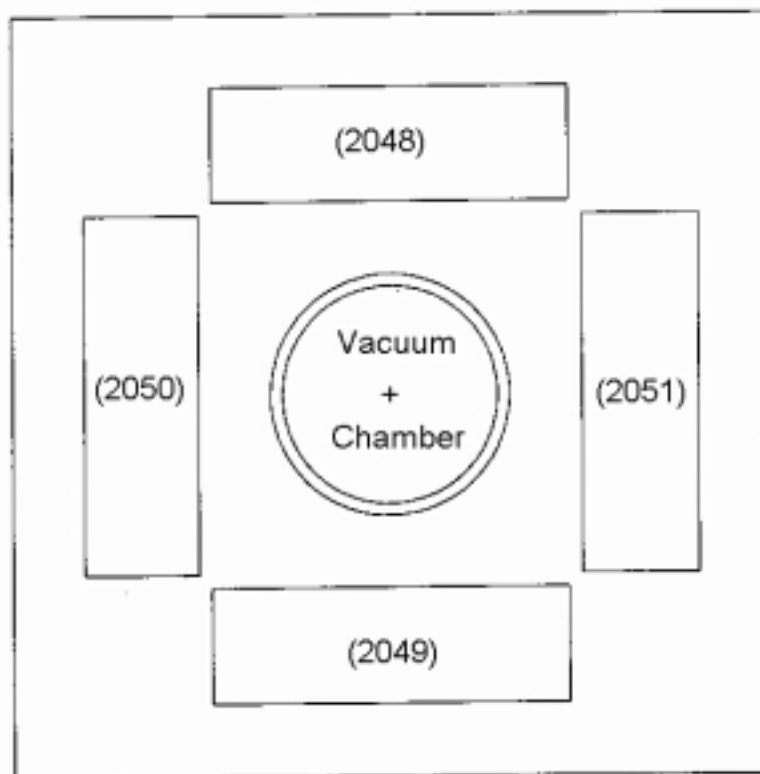


Figure 4: Cross Section Through Cells in Which Dose is Determined (First Quadru-Pole - Cell Number in Parenthesis)

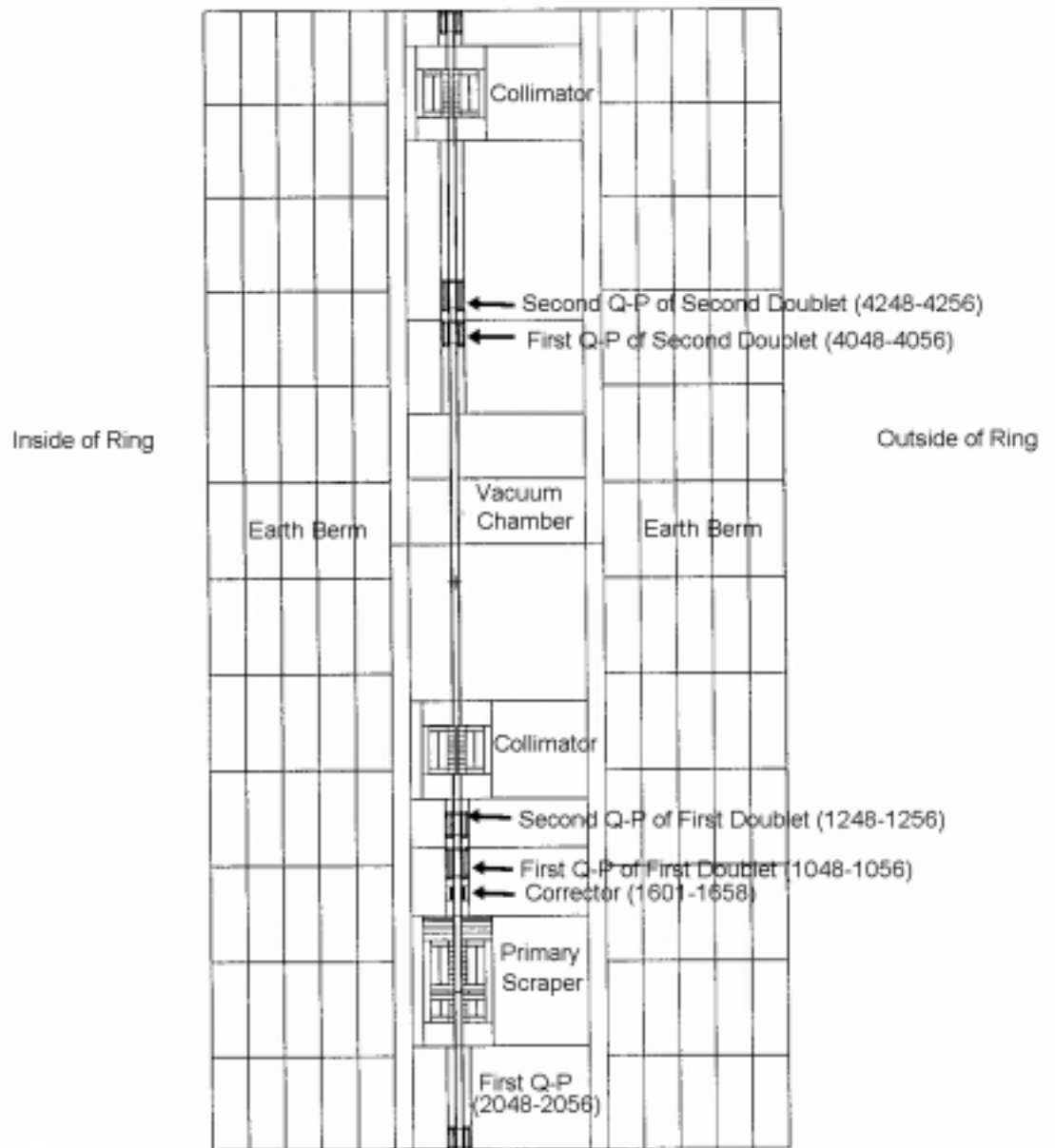


Figure 5: Longitudinal Section Along Collimation Straight of Ring at Level of Vacuum Chamber
 (Number in parenthesis correspond to magnet cell number used in tables)

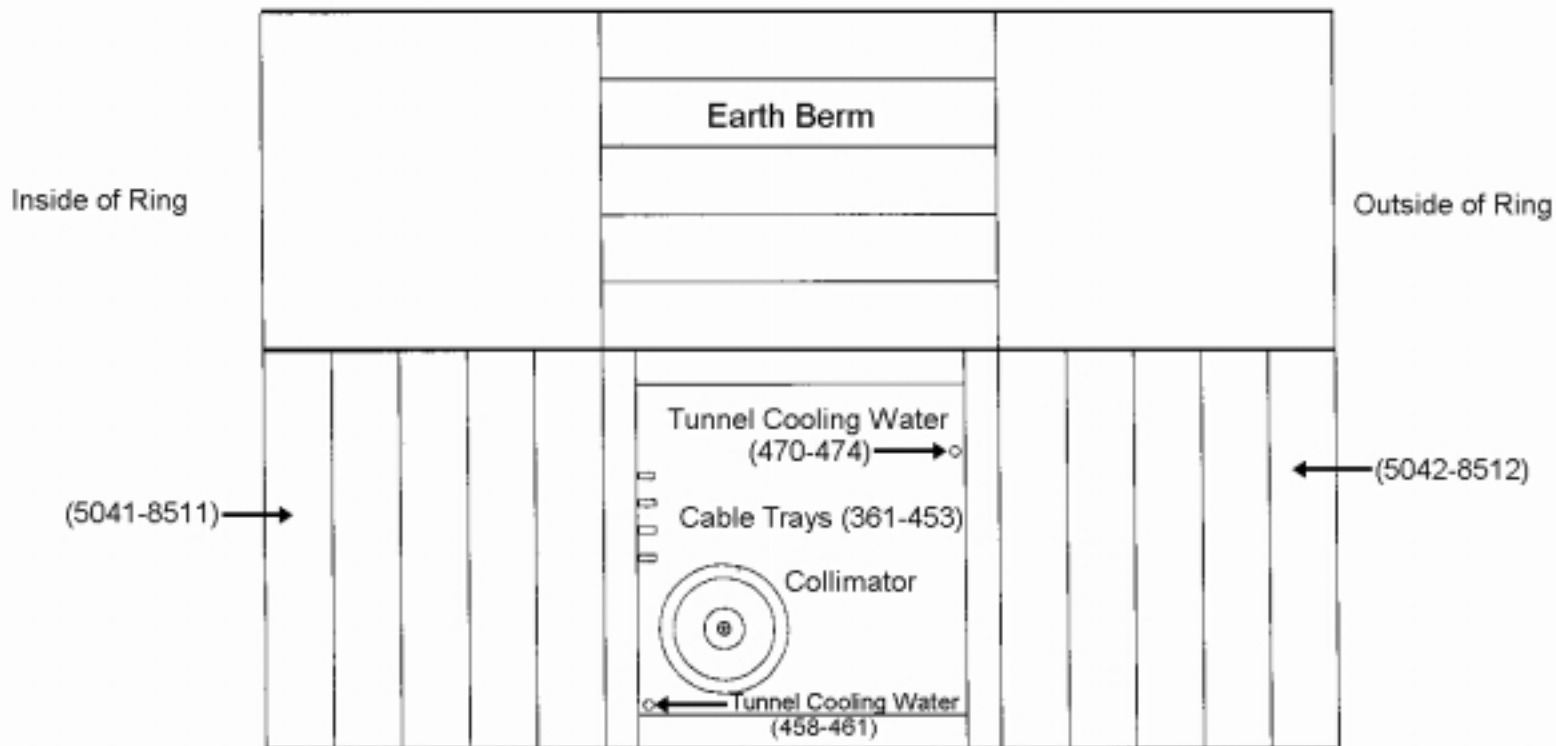


Figure 6: Cross Section Through Ring at Location of Primary Scraper
 (Numbers in parenthesis correspond to cell numbers used in tables)

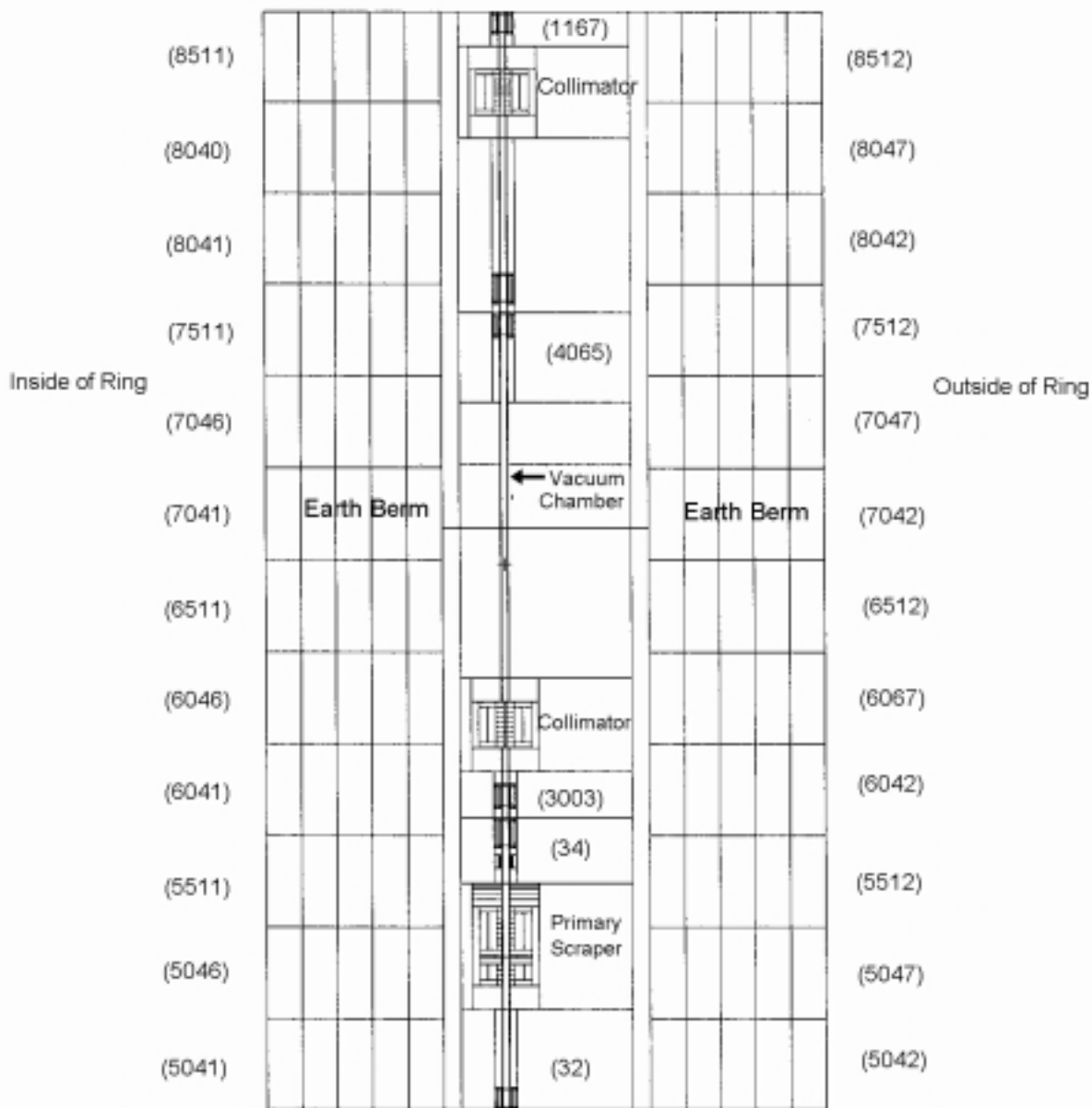


Figure 7: Longitudinal Section Along Collimation Straight of Ring at Level of Vacuum Chamber (Numbers in parenthesis correspond to earth berm and tunnel air cell numbers used in tables)